RAPID COMMUNICATIONS

PHYSICAL REVIEW B VOLUME 48, NUMBER 17 1 NOVEMBER 1993-I

Flux-front motion parallel to CuO_2 planes in $YBa_2Cu_3O_{7-\delta}$ observed with a scanning Hall probe

D. A. Brawner* and N. P. Ong
Joseph Henry Laboratories of Physics, Princeton University, Princeton, New Jersey 08544

Z. Z. Wang
Lab 2M/CNRS, 196 avenue Henri Ravéra, 92220 Bagneux, France

(Received 16 August 1993)

The motion of the flux front in $YBa_2Cu_3O_{7-\delta}$ with the field applied parallel to the layers is studied using a scanning Hall probe. By tracking the peak positions versus field in the remanence, we determine directly the critical current density perpendicular to the layers ($J_c^{\perp}=8.3\times10^4$ A/cm^2 at 4.2 K). The observed critical-current anisotropy (~500) is much larger than indicated by high-temperature measurements. By scanning the flux profiles in the direction perpendicular to the layers, we find direct evidence that flux motion occurs parallel to the layers. A model that accounts for the observed mountain-pass topography in the remanence is presented.

The layered structure of the cuprate superconductors leads to strong anisotropy in the vortex motion.[1] Although the anisotropy of quantities such as the critical transport current has been intensively studied at temperatures near the transition temperature T_c, much less is known about the low-temperature anisotropy, especially with the field aligned parallel to the layers. In this field geometry, calculations[2] suggest that vortices sit in deep potential troughs created by the modulation of the order parameter along the c axis. Motion along the troughs is relatively unimpeded whereas motion parallel to **c** is opposed by a large energy barrier. The aim of our experiment is to study vortex motion in this geometry in 90 K $YBa_2Cu_3O_{7-\delta}$, using a scanning Hall probe to image directly motion of the flux front. Roas, Schultz, and Saemann-Ischenko[3] (RSS) report that, in thin-film $YBa_2Cu_3O_{7-\delta}$ at 4.2 K, the critical current density parallel to the CuO_2 layers with $\mathbf{H}\perp\mathbf{c}$ is ~10 times larger than with $\mathbf{H}\|\mathbf{c}$. However, the value of J_c in the direction *perpendicular* to the layers (corresponding to vortex motion along the troughs) has not been measured. We demonstrate that the scanning probe technique enables a direct measurement of $J_c^{\perp}$ (the critical current density parallel to **c**) without assumptions on the flux distribution (such as in the Bean model[4]). We present evidence for an anisotropy that is so large that the motion of vortices is essentially one dimensional in this geometry. Unexpectedly, the observed remanence consists of two prominent peaks bracketing a mountain-pass feature. The latter feature is produced by an interesting instability in the advancing flux front, which we account for by slightly generalizing the one-dimensional model of Vinokur, Feigel'man, and Geshkenbein (VFG).[5]

The Hall probe is comprised of a thin bismuth film lithographically etched into a Hall device with an active area of 2×4 μm^2. With a probe current of 0.3 mA, the device can resolve 0.3 G in a background field of 7 T.[6] The probe is scanned slowly (1–3 μm/s) at a height Δz above the *ac* face of the crystal. By comparing the scan taken in the Meissner state with the field distribution around a perfectly screened sample of ellipsoidal geometry, we estimate Δz to be 10 μm. The *ab* face is of dimension 600×400 μm^2 while the thickness along **c** is 150 μm. Because of the heavy twinning, we will not distinguish the a axis from the b axis. As shown in the inset in Fig. 1, we take $\hat{\mathbf{x}}\|\mathbf{a}$, $\hat{\mathbf{y}}\|\mathbf{c}$, and $\mathbf{H}\|\hat{\mathbf{z}}$. At any stage of the magnetization cycle, the Hall-probe signal is proportional to the z component of the local induction (hereafter called B). The large dimension of the crystal (400 μm) along the field direction makes demagnetization effects unimportant.[7]

The sample is cooled in zero field (all scans are taken at 4.2 K). After the field is increased to some value H, a scan is performed, either parallel to perpendicular to the layers (along $\hat{\mathbf{x}}$ or $\hat{\mathbf{y}}$, respectively). These "in-field" scans capture the variation of the flux density B with x. The field is then returned to zero, and a scan repeated to image the trapped flux (the "remanence profile"). The two scans are repeated at successively higher fields. We discuss first the scans parallel to the layers. The in-field scans in Fig. 1 show profiles of the flux density B, with H fixed at the values indicated (the $B=0$ level is suppressed). The sharp decrease in B for the scan at the lowest field locates the flux-front position. As flux penetrates further into the crystal along $\pm\mathbf{x}$ with increasing H, the gradient of the front decreases significantly (compare, especially, the left fronts for $H=430$ Oe with the ones at fields above 810 Oe). The asymmetry in the scans arises from a slight misalignment which makes Δz increase slightly with x. The magnetization M, given by the "depth" of the minimum relative to the value of B outside the sample, also may be seen to increase in magnitude between 430 Oe and 2530 Oe. Above 2530 Oe, it gradually decreases with increasing field in a way characteristic of M vs H curves. In principle, the critical current $J_c^{\perp}$ may be determined from the slope dB/dx. However, this is unreliable because the scale factor s that relates the Hall-probe signal to the actual value of B

within the sample is difficult to calculate reliably in the mixed state (s decreases if Δz increases).[6] Instead, we adopt the technique of tracking the position of the peaks in the remanence. The remanent profiles parallel to the layers (Fig. 2) display the double-peak structure reminiscent of the Bean model. It is clear that, with increasing field, the two peaks move closer and eventually coalesce. As in the usual critical-state picture, the peak positions denote the depth (measured from the nearest edge) to which vortices are swept out when the field is ramped to zero. Within our uncertainty, we find that the peak position x_p varies linearly with H. A straight-line fit to the data enables us to determine $J_e^{\perp}=(dH/dx_p)/2$, *without knowing* s. The value of $J_c^{\perp}$ is found to be 8.3×10^4 A/cm^2. This $J_c^{\perp}$, together with the length of the crystal (600 μm) implies that the remanence should saturate (merge into a single peak) at an applied field of 6 kOe, i.e., the fronts meet at the center at the characteristic field $H_{\parallel}^{*}\sim3$ kOe. We have confirmed this by direct measurement (not shown in Fig. 2). In previous experiments,[6] we performed a similar determination of J_c with **H** aligned perpendicular to the layers. (With **H**$\|$**c**, the critical-state current, denoted by J_c^{ab}, flows entirely within the *ab* plane.) There, we found that J_c^{ab} equals 4×10^6 A/cm^2 at 4.2 K. Thus, $J_c^{\perp}$ is approximately 50 times smaller than J_c^{ab}. Actually, the current anisotropy relevant to our geometry is even larger. With field parallel to the layers, the critical-state current has components perpendicular and parallel to the layers. The former is $J_c^{\perp}$, whereas the latter (which we call $J_c^{\parallel}$) opposes vortex motion *perpendicular* to the layers. In the experiment of RSS,[2] $J_c^{\parallel}$ is found to be ~10 times larger than J_c^{ab} at 4.2 K. This ratio implies that $J_c^{\parallel}\sim4\times10^7$ A/cm^2 in our crystal. Thus, with **H** parallel to the layers, the ratio $J_c^{\parallel}/J_c^{\perp}$ is of the order of 500. This extreme anisotropy, much larger than indicated by previous experiments at temperatures near T_c, shows that the intrinsic barrier, in fact, dominates vortex pinning and motion at low temperatures. Wu and Sridhar[8] infer from *ac* penetration depth measurements a critical current anisotropy of ~10. We note that their ratio (five times less than our $J_c^{ab}/J_c^{\perp}$) is deduced from a simple linear-response model for vortex displacement, whereas the present measurements probe directly motion of the flux front.

If flux enters and leaves the crystal in the direction perpendicular to the layers, we should expect the corresponding in-field and remanence profiles to be similar to those in Figs. 1 and 2. Instead, we find that they are qualitatively different. Figure 3 displays in-field scans of B (zero suppressed) taken along **c** through the center of the *ac* face. The steepness of the flux fronts does not change appreciably with increasing field. Moreover, the magnetization profiles for the three highest fields in Fig. 3

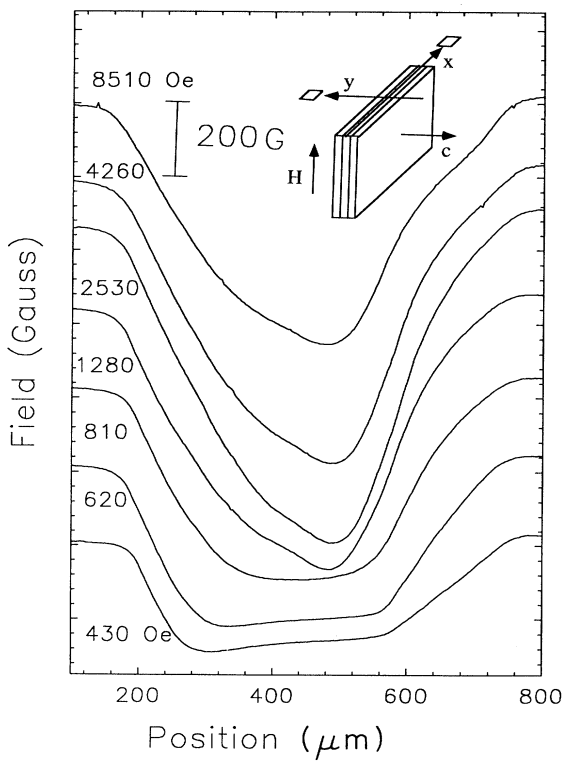

FIG. 1. Scans of flux density B vs x parallel to layers at the fixed fields H (as indicated) in $YBa_2Cu_3O_{7-\delta}$ crystal at 4.2 K (zero suppressed). The decrease in slope with increasing H reflects flux penetration along $\pm$**x**. The inset shows the scan directions and the field orientation. The top surface is called the *ac* face in the text.

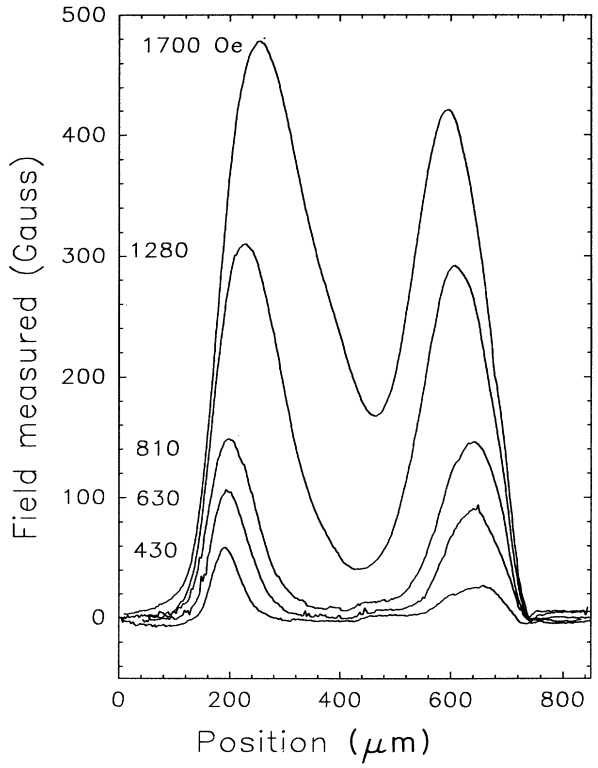

FIG. 2. Remanence profiles scanned parallel to layers (along **x**) after the field is increased to the maximum value indicated. The two-peak structure is caused by flux expulsion along $\pm$**x**. The linear variation of x_p vs H determines $J_c^{\perp}$ to be 8.3×10^4 A/cm^2.

are very similar in shape and magnitude. From these features we draw two inferences. Rather than advancing into the crystal, as in the parallel case, the fronts, when scanned along **c**, *remain pinned* to the edges of the crystal. However, it is readily seen from the scans that the magnetization (depth of the minimum) is insensitive to H. This means that the flux density in the middle of the *ac* face increases with field as $H - H_0$, with H_0 a constant field, i.e., flux is penetrating to the middle of the crystal. Together, the two inferences imply that the direction of vortex motion is not along **c**, but in the direction parallel to the layers.

This is strikingly confirmed by the remanence profiles taken along **c** (Fig. 4). In contrast to the remanent profiles in Fig. 2, these scans (through the center of the *ac* face) show no trace of the two-peak structure. Instead, only one peak is observed in the remanence for all fields between 430 Oe and 50 kOe. (Recall that in Fig. 2 the single-peak remanence is observed only if H exceeds $2H_{\parallel}^{*} \sim 6$ kOe.) Combining these scans with those in Fig. 2, we infer that the remanence resembles two prominent peaks separated by a mountain pass, as sketched in Fig. 4.

In an anisotropic superconductor exposed to a field H, the usual Bean picture is that the flux penetrates to distances H/J_{cy} and H/J_{cx} along the x and y axes, respectively. When the field is removed, half the flux is expelled, so that the remanent magnetization displays a ridge that completely surrounds the center of the *ac* face (we assume that the flux does not penetrate to the center of the crystal in either direction). Just as in the isotropic case, the ridge separates the interior, in which the current is (say) clockwise, from the exterior region in which **J** is counterclockwise. Thus, a scan along either the x or y axes should reveal a double-peak structure.

As discussed above, this expectation disagrees with the scans in Fig. 4. We note further that the observed mountain-pass topography implies that **J** is counterclockwise *everywhere*. To understand the new features, we examine how the one-dimensional (1D) vortex motion is influenced by the current distribution which is, at least, two dimensional (2D). As discussed below, this interplay introduces an instability that causes the invading flux front to be strongly curved, instead of being planar, i.e., vortices in the midpoint of the flux front diffuse much faster than those near the sides. When the applied field is increased to H, vortices penetrate by diffusing parallel to the planes. The flux gradient along **x** is determined by

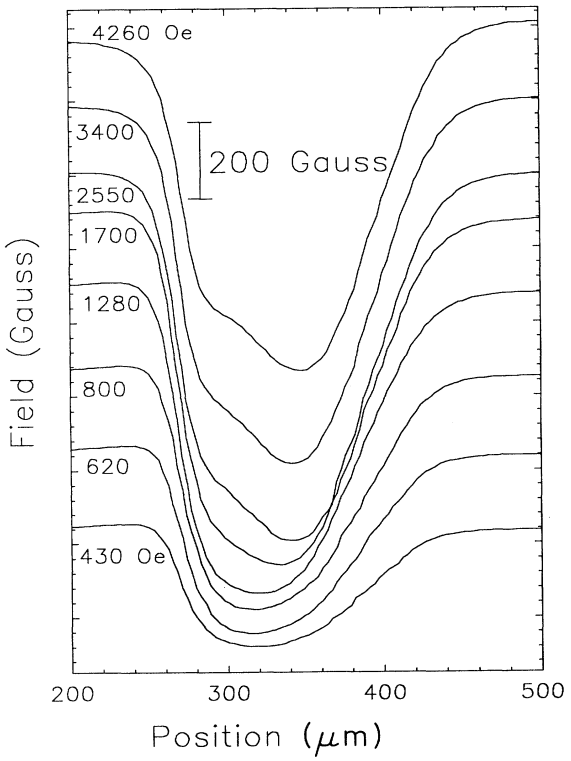

FIG. 3. Profiles of B vs y (scanned perpendicular to layers) for fields fixed at the values indicated (zero suppressed). For the four highest fields, the magnetization profiles are similar in shape and magnitude. Unlike the curves in Fig. 1, the flux fronts are not observed to move into the sample (along $\hat{\mathbf{y}}$).

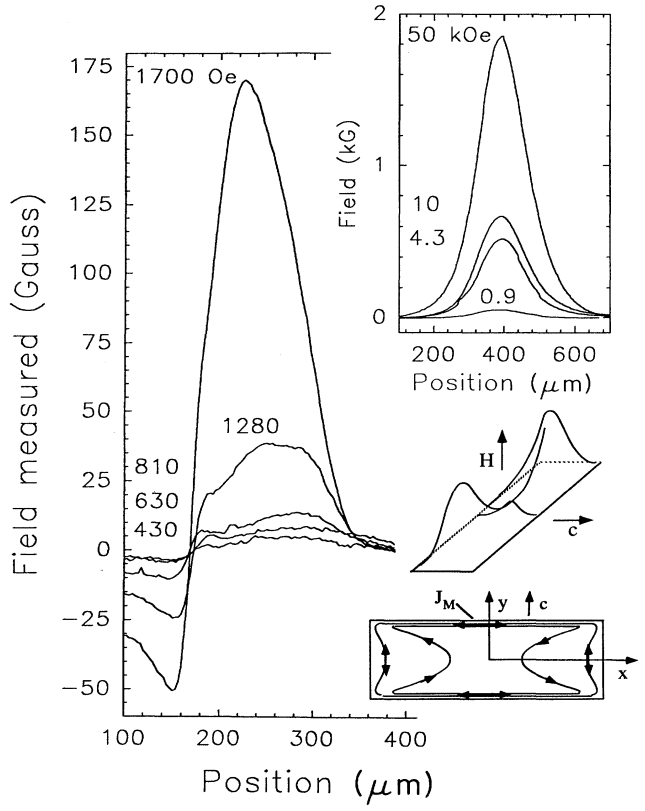

FIG. 4. (Main panel) Remanence profiles scanned along **c** through the center of the *ac* face after H is increased to the values indicated. The top inset on the right shows similar profiles taken for higher values of H on the same crystal. The middle inset on the right shows the mountain-pass topography of the remanence. The lowest inset depicts the proposed current paths in the xy plane. During the invasion phase **J** is clockwise in both the inner and outer closed loops. In the expulsion phase J_M (the reversible surface current on the *ab* faces) and the bulk current in the outer loop reverse direction (bidirectional arrows). The bulk current in the inner loop, however, remains unchanged (unidirectional arrows).

the effective critical-state current $J_c^{\perp}$. Along **y**, however, the steep gradient is maintained by a much larger Meissner "surface current" J_M on the *ab* faces that prevents any vortex penetration as sketched in the lowest inset in Fig. 4 ($J_M \sim H/\lambda_{ab}$ where λ_{ab} is the penetration depth). An essential feature of J_M is that it is completely reversible, unlike the critical-state currents in the interior. Moreover, the flux-front instability leads to much faster vortex diffusion at the midplane than at the sides. Thus, in a scan along **y** the minimum in the flux density does not occur at the center, but at two points near the edge. (The high-field scans in Fig. 3 show evidence for the double-well minima despite the skewing caused by variation of the sensor scan-height.) The pronounced curvature of the flux front and the large value of J_M lead to the "anvil" pattern for the current distribution, as depicted in the lowest inset in Fig. 4.

Next, as the field is decreased to zero, vortices are expelled in the direction parallel to the layers. On the *ab* faces, J_M reverses direction. However, in the interior, the critical-state current reverses direction only within a strip of width $H/J_c^{\perp}$ near the surface (outer current loop in the lowest inset in Fig. 4). Everywhere else the flux density and the current distribution are unaffected (inner loop). It is readily seen that this results in (i) a current pattern that is counterclockwise everywhere and (ii) a remanence that resembles a mountain pass bracketed by two prominent peaks. The single-peak profiles in Fig. 4 simply reflect the deeper penetration of the vortices in the midplane compared with the sides during the invasion phase of the experiment.

Finally, we discuss the origin of the instability of the invading flux front. In the 2D approximation where $\mathbf{B}=B(x,y)\hat{\mathbf{z}}$ and the vortex velocity $\mathbf{v}=v(x,y)\hat{\mathbf{x}}$, the induction law simplifies to $\partial B(x,y)/\partial t=-\partial(Bv)/\partial x$. At low temperatures where vortex motion is activated, the velocity is a highly nonlinear function of the x component of the driving Lorentz force J_yB. Generalizing the 1D model of Vinokur, Feigel'man, and Geshkenbein[5] to accommodate a 2D current, we have $v(x,y)=v_0(J_y/J_c^{\perp})|J_y/J_c^{\perp}|^{\sigma}$ where v_0 sets the hopping velocity scale and the exponent σ equals U_0/k_BT.[9] For small changes in B, the induction law reduces to a diffusion equation $\partial B/\partial t=-\partial[D(J_y)\partial B/\partial x]/\partial x$, with a current-dependent diffusion coefficient

$$D(J_y)=(Bv_0/\mu_0 J_c^{\perp})|J_y/J_c^{\perp}|^{\sigma} \quad (1)$$

(μ_0 is the free-space permeability). At 4.2 K, σ is estimated from relaxation of the magnetization to be larger than 30 (this is for the geometry with **H**||c, however).[10]

The strong dependence of the diffusion coefficient on J_y implied by Eq. (1) and the boundary conditions on the current distribution are sufficient to produce an instability in the flux front. At the boundaries of the xy plane (i.e., on the *ab* faces), the vortex diffusion rate is strongly suppressed since J_y must be zero. Suppression of the diffusion rate at the boundaries causes an advancing flux front that is initially planar to develop curvature, as sketched in the inset in Fig. 4. Because **J** follows the contour of B, curving of the front reduces J_y everywhere relative to its value at the midplane (where J_x is zero by symmetry). The nonlinear dependence of $D(J_y)$ on J_y [Eq. (1)] strongly amplifies this difference, thereby greatly enhancing the diffusion rate in the midplane relative to the sides. In turn, this leads to a further increase in the curvature of the front. Thus, the 2D boundary conditions for **J** and the sensitivity of $D(J_y)$ to J_y together cause the planar flux front to be unstable towards developing strong curvature.

In summary, we have used a scanning Hall microprobe to track the progress of the flux front when a field is aligned parallel to the layers in $YBa_2Cu_3O_{7-\delta}$. At 4.2 K, the critical current anisotropy (~ 500) is much larger than expected, implying that the vortex motion is one dimensional. For vortex motion parallel to the layers, the relevant critical current $J_c^{\perp}$ is still quite considerable (8×10^4 A/cm^2). The topography of the remanence, two peaks separated by a saddle point, is qualitatively different from that expected from the usual Bean picture. We account for the unexpected remanent profile by adapting the VFG model for vortex diffusion with a strongly current-dependent diffusion coefficient. The model also shows that the advancing flux front is unstable towards developing strong curvature. We argue that this instability, together with the reversible nature of the surface currents on the *ab* faces, results in the observed mountain-pass remanence.

We acknowledge support from the U.S. Office of Naval Research (Contract No. N00014-90-J-1013.P2), the Seaver Institute, and Defense Advanced Research Projects Administration (by subcontract from the Texas Center for Superconductivity, University of Houston).

*Present address: Lab für Festkörperphysik, ETH-Hönggerberg, CH-8093 Zürich, Switzerland.

[1]For a survey, see Physica C **185-189**, 3 (1991).

[2]M. Tachiki and S. Takahashi, Solid State Commun. **70**, 291 (1989); D. Feinberg and C. Villard, Phys. Rev. Lett. **65**, 919 (1990); John R. Clem, Phys. Rev. B **43**, 7837 (1991).

[3]B. Roas, L. Schultz, and G. Saemann-Ischenko, Phys. Rev. Lett. **64**, 479 (1990).

[4]C. Bean, Phys. Rev. Lett. **8**, 250 (1962).

[5]V. M. Vinokur, M. V. Feigel'man, and V. B. Geshkenbein, Phys. Rev. Lett. **67**, 915 (1991).

[6]D. A. Brawner, N. P. Ong, and Z. Z. Wang, Nature **358**, 567 (1992); D. A. Brawner and N. P. Ong, J. Appl. Phys. **73**, 3890 (1993).

[7]The small estimated demagnetization factor ($L_z \sim 0.12$) implies that the field at the sample edge is enhanced by at most $\sim 10\%$ in the *Meissner* state ($H < H_{c1}$). In the remanent state, spreading of the flux lines is expected, as they emerge from the interior to the plane of the Hall sensor. This affects the factor s. However, in the yz plane scans (Figs. 3 and 4), this spreading is strongly suppressed by the large intrinsic-barrier pinning which tends to keep flux lines parallel to the layers.

[8]Dong-Ho Wu and S. Sridhar, Phys. Rev. Lett. **65**, 2074 (1990).

[9]VFG (Ref. 5) assume an activated velocity of the form $v=v_0(J/J_c)\exp[-U(J)/k_BT]$, with a potential that decreases logarithmically with J, viz., $U(J)=U_0\ln|J_c/J|$.

[10]D. A. Brawner, N. P. Ong, and Z. Z. Wang, Phys. Rev. B **47**, 1156 (1993).